Percolation in the hypercube and the Ising spin-glass relaxation

B. Kahng
Center for Polymer Studies and Department of Physics, Boston University, Boston, Massachusetts 02215
*and Department of Chemistry, University of California, Berkeley, California 94720**
(Received 28 August 1990)

We investigate percolation clusters in a d-dimensional hypercube of linear dimension 2. This set can be used to describe the configurational space of an Ising spin-glass system. We derive the perimeter polynomials for general dimensions and expand in powers of $1/\eta$, where $\eta=d-1$ and the coordination number is d. The leading term in the series expansion yields the Bethe approximation. In a finite dimension, a crossover occurs from scaling to homogeneous behavior in a finite region above the percolation threshold. In the scaling region, finite-dimensional scaling is considered for the cluster size distribution by applying a phenomenological renormalization-group argument. For the percolation clusters we consider the mean Hamming distance of random walks; this quantity corresponds to the Ising spin-glass order parameter. This configuration-averaged Hamming distance shows (i) a stretched exponential relaxation $(p-p_c)^{-a}t^{-x}\exp[-(t/\mathcal{T})^{\beta}]$ with $\mathcal{T}\sim(p-p_c)^{-z\nu}$ as $p\to p_c^{+}$ with the exponents $a\sim\frac{3}{5}$, $x\sim\frac{1}{6}$, $\beta=\frac{2}{5}$, $z\nu=3$; and (ii) an extremely slow relaxation at $p=p_c$, in infinite-dimension limit. This result illustrates Ogielski's numerical simulation data [Phys. Rev. B **32**, 7384 (1985)] in an Ising spin-glass system.

I. INTRODUCTION

The phenomenon of stretched exponential relaxation in spin-glass systems has been the focus of considerable attention.[1-6] In addition to occurring in spin glasses, this stretched exponential relaxation arises in diverse situations such as, e.g., in the autocorrelation function of the structure factor of polymer chains,[7] or in the kinetics of trapping reactions,[8] etc. In Ising spin glasses, it is the Edwards-Anderson order parameter, $q(t)$, that exhibits a stretched exponential relaxation near the glass temperature,

$$q(t)\sim t^{-x}\exp[-(t/\mathcal{T})^{\beta}]\ , \tag{1}$$

where $0<\beta<1$, and $\mathcal{T}$ is the characteristic relaxation time. Many theoretical approaches to describe this behavior have been undertaken. For example, Palmer *et al.*[2] have considered the hierarchical model and derived stretched exponential decay depending on the weight distribution. Ogielski[6] has performed Monte Carlo simulation in an Ising spin glass, and obtained the stretched exponential decay phenomenologically in which the exponents x and β depend on temperature, and the characteristic relaxation time diverges as temperature approaches the critical temperature. Recently experimental measurements[9] on $Fe_{0.5}Mn_{0.5}TiO_3$ for the order parameter, $q(t)$, are also in good fit with the Ogielski's simulation result. A study of infinite-range mean-field theory[10] of spin glasses has been also considered, but it does not agree with experimental data.

Recently a very appealing picture of spin-glass relaxation has been proposed by Campbell *et al.*,[11] in which the evolution of the Edwards-Anderson order parameter is mapped into the dynamics of a random walk on percolation clusters which are embedded in high-dimensional hypercubes of linear dimension 2. The hypercube contains 2^d vertices which represent the configurations of a system containing d Ising spins. The mean Hamming distance of the random walk from its starting position corresponds to the Edwards-Anderson order parameter, where the Hamming distance is defined as the shortest distance on the underlying undiluted lattice. Moreover the percolation disorder mimics energy disorder in spin-configuration states of the Ising spin-glass system. This connection will be reviewed in Sec. II. Numerical simulations[11] indicate that the mean displacement decays to its equilibrium values according to the stretched exponential decay given in Eq. (1), with a probability dependent exponent, β, that equals $\frac{1}{3}$ at the percolation threshold p_c and with $\mathcal{T}\to\infty$ as $p\to p_c$. This exponent value appears to be consistent with the estimate obtained in Ogielski's simulations of Ising spin glasses. Recently Bray and Rodgers[12] have considered diffusion on percolation clusters embedded in a hypertetrahedron as a model for spin-glass relaxation. They found stretched exponential relaxation for the probability of return to the origin, with the exponent $\beta=\frac{1}{3}$ for all values of p. This result was derived assuming that percolation clusters on the hypertetrahedron are quasi-one-dimensional. In our work, we find, however, that branching of clusters plays an important role for percolation on the hypercube. Therefore we argue that the percolation clusters on hypercube cannot be regarded as quasi-one-dimensional.

In this paper, we investigate the behavior of random walks on percolation clusters which are embedded in a d-dimensional hypercube of linear dimension equal to 2, a 2-hypercube. In addition to the connection to Ising spin glasses, there is intrinsic interest for understanding the geometry of percolation clusters in a confined space. For

studying this percolation problem, we first employ exact enumeration to derive the perimeter polynomials that characterize the cluster size distribution on 2-hypercubes of various dimensionalities. Owing to the restriction to linear dimension 2, exact enumeration provides considerable information about the cluster structure on the hypercube. From the enumeration data, we derive the perimeter polynomials for general spatial dimension d and we derive series in powers of $\eta=1/(d-1)$, where d is also the coordination number on the hypercube. The leading term in this type of series coincides with the Bethe approximation, while the leading and the first-order correction agree with the corresponding series terms in the high-dimensional series expansion for percolation on an infinite lattice. We also use the enumeration data to develop a finite-*dimensional* scaling ansatz, which is analogous to finite-*size* scaling for a large system at its critical point.

The dynamics of random walks on these percolation clusters is considered next. From the purely exponential decay of the probability distribution of a random walk on a fixed one-dimensional interval, a stretched exponential relaxation emerges upon averaging over all interval lengths. Similarly for a finite-size fractal structure, the long time relaxation of a random walk is purely exponential, with the characteristic decay time determined by the fractal dimension of the random walk, d_w. For percolation clusters on the hypercube, there is a broad distribution of cluster sizes and correspondingly broad distribution of relaxation times. Thus by averaging the pure exponential decay over the cluster size distribution, we obtain the stretched exponential relaxation of the form given in Eq. (1) for $p \to p_c^+$. Also we obtain the exponents $\beta=\frac{2}{5}$ and $x \sim \frac{1}{6}$ in infinite dimension, which corresponds to the thermodynamic limit. Our result seems to be reasonable with the estimated Ogielski's numerical simulation values in the Ising spin-glass system near the critical temperature.

The paper is organized as follows. In Sec. II, we introduce the random-walk model on the 2-hypercube and explain the connection to Ising spin glasses. In Sec. III, the geometry of percolation clusters embedded in the hypercube is examined using exact enumeration, together with developing an asymptotic expansion for the high-dimensionality limit. In order to compare the numerical simulation results of random walks performed in finite dimension,[11] we consider the cluster size distribution numerically in finite dimension in Sec. IV based on exact enumeration and Monte Carlo data. In Sec. V, we present the solution for the relaxation of one-dimensional random walks and then study the corresponding relaxation of random walks on percolation clusters in the hypercube in Sec. VI. From this investigation, we obtain predictions for the nature of the relaxation function. The final section is devoted to the conclusions.

II. CONNECTION BETWEEN AN ISING GLASS AND RANDOM WALKS

Consider an Ising spin glass with nearest-neighbor interactions which can take on the values $\pm J$ with probability $\frac{1}{2}$. The temporal evolution of the spins is taken to follow the single-spin-flip Monte Carlo simulation method as discussed in Ref. 6. The configurational average of the spin autocorrelation function gives the Edwards-Anderson order parameter $q(t)=\sum_x \overline{\langle S_x(0)S_x(t)\rangle}$. Here the angle brackets represent an average over all temporal evolutions and the overbar denotes an average over the random bond configurations.

For a given configuration of bonds and for a given temporal evolution the spin autocorrelation function can be written as

$$\tilde{q}(t)=\sum_x S_x(0)S_x(t)=N_{\uparrow\uparrow}-N_{\uparrow\downarrow}=N-2N_{\uparrow\downarrow}\ , \qquad (2)$$

where $N_{\uparrow\uparrow}$ ($N_{\uparrow\downarrow}$) represents the number of spins having the same (opposite) orientation at time $t=0$ and at time t, and N is the total number of spins in the system. Since each spin has two states, the total number of configurations is 2^N, each of which can be represented as a corner of an N-dimensional hypercube of linear size 2, a 2-hypercube. We define the distance between two corners of the hypercube, a and b, as the minimum number of the edges needed to connect a and b. This measure is the Hamming distance, and it counts the number of spins that have different orientations in two distinct configurations which are represented by different corners in the cube. If two corners represent the spin configurations with time difference t, the distance between the corners, denoted as $r(t)$, equals the number of spins with different spin orientations $N_{\uparrow\downarrow}$. Hence $\overline{\langle r(t)\rangle} \sim \overline{\langle N_{\uparrow\downarrow}\rangle}$, and the time-dependent part of the order parameter $q(t)$ corresponds to the relaxation of random walks $\overline{\langle r(\infty)\rangle - \langle r(t)\rangle}$. For the 2-hypercube, the Hamming distance is also equivalent to the square of the Euclidean distance. Notice that the Hamming distance is different from the chemical distance, which is defined as the shortest distance between two points on a cluster.

Suppose that each site of the hypercube is randomly occupied with probability p, and consider the dynamics of a random walk on the percolation clusters that are formed. Each step of the walk is equivalent to flipping one spin in the corresponding spin configuration. The possibility of a spin flip in a Monte Carlo simulation is determined by the value of a local exchange field acting on the spin. The percolation occupation probability mimics the disorder in the local field value. Since the value of the local field depends on temperature, the site occupation probability is related to temperature. We presumably regard the percolation threshold as the critical point, the glassy temperature. However, the model of random walk on percolation clusters is a naive picture of the Ising spin-glass dynamics, because percolation disorder is purely random, while the spin-glass disorder has a correlation between spin configurations. Nevertheless, it is worthwhile to consider the percolation model as a simple model to understand the dynamics of the Ising spin-glass system.

III. PERCOLATION ON THE HYPERCUBE

To investigate percolation on the hypercube, we have modified an enumeration program[13] to calculate the num-

ber of clusters and the number of associated perimeter sites on the 2-hypercube for up to nine sites for spatial dimension $d \leq 9$. These computations required approximately 2.5 h of CPU time on an IBM 3090 computer. We then followed the steps outlined by Gaunt, Sykes, and Ruskin[14] (GSR), for percolation in an infinite system in high-dimensionality limit, to calculate the first nine terms in the general-d series for the perimeter polynomials, $\tilde{D}_s(p,d)$, as defined in Eq. (3) below.

Since we are ultimately interested in finding probability to have an s-site cluster which is connected to the origin, it proves convenient to define the perimeter polynomials in terms of the first moment of the cluster size distribution as

$$\sum_s s n_s(p,d) \equiv \sum_s \tilde{n}_s(p,d) = \sum_s s \sum_t g_{st} p^s (1-p)^t \equiv \sum_s p^s \tilde{D}_s(p,d) \ . \tag{3}$$

Here g_{st} is the number of animals containing s sites and t perimeter sites on the hypercube, $n_s(p,d)$ is the average number of s-site clusters per site when each site is occupied with probability p, and $q=1-p$. The perimeter polynomial that we employ, $\tilde{D}_s(p,d)$, corresponds to $sD_s(p,d)$, of the conventional perimeter polynomial. The data for the perimeter polynomials are presented in the Appendix.

We have also computed the number of s-site lattice animals, $\tilde{N}_s(d)$, and the series coefficients for the mean cluster size, $S(p)$, on the hypercube. Following the notation of GSR, these can be written in the form

$$\tilde{N}_s(d) = \sum_{\xi=1}^{s-1} A_\xi^s \begin{bmatrix} d \\ s-\xi \end{bmatrix} = s^{s-2} \begin{bmatrix} d \\ s-1 \end{bmatrix} + \tfrac{1}{2} s^{s-4}(s-2)(s-3)^2 \begin{bmatrix} d \\ s-2 \end{bmatrix} + \cdots \tag{4}$$

and

$$S(p) = \sum_s s \tilde{n}_s(p,d) \equiv \sum_s b_s p^s \ . \tag{5}$$

Substituting $q=1-p$ into the perimeter polynomials, the series coefficients b_s are

$$b_s(d) = \sum_{\xi=0}^{r-1} B_\xi^s \begin{bmatrix} d \\ s-\xi \end{bmatrix} = s! \begin{bmatrix} d \\ s \end{bmatrix} + \tfrac{1}{2}(s-1)!(s-2)(s-4) \begin{bmatrix} d \\ s-1 \end{bmatrix} + \cdots \ . \tag{6}$$

For fixed d, the series for $\tilde{N}_s(d)$ and b_s differ from the terms in the corresponding series for ordinary percolation due to the restriction of the system to a hypercube.

We can now derive the general-d form of the series for the hypercube by applying the general methods developed by Fisher and Gaunt.[15] For this purpose, we write the series coefficients in powers of the parameter $1/\eta$. This expansion parameter, $1/\eta$, is essentially the inverse effective coordination number for the hypercube. Hence in a d-dimension hypercube, the expansion parameter equals $1/\eta = 1/(d-1)$, rather than $1/(2d-1)$. We first write the binomial coefficient $\binom{d}{s}$ in powers of $1/\eta$ as[15]

$$\begin{bmatrix} d \\ s \end{bmatrix} = \frac{\eta^s}{s!} \left[1 - \frac{1}{2\eta} s(s-3) + \frac{1}{24\eta^2} s(s-1)(s-2)(3s-13) + \cdots \right] . \tag{7}$$

Substituting Eq. (7) into Eq. (4) leads to general-d expression for the number of animals

$$\tilde{N}_s(d) = \frac{s^{s-2}\eta^{s-1}}{(s-1)!} \left[1 - \frac{(s-1)(4s^2-21s+18)}{2s^2} \eta^{-1} + \cdots \right] . \tag{8}$$

Using Stirling's approximation, this can be written as

$$\tilde{N}_s(d) \sim A s^{-3/2} e^{-as} \ , \tag{9}$$

where A is a constant, and $a = -(1+\ln\eta)$. Similarly, we also obtain b_s as an expansion in $1/\eta$ by substituting Eq. (7) into (6) to yield

$$b_s(d) = \eta^s [1 - (\tfrac{3}{2}s - 4)\eta^{-1} + \cdots] \ . \tag{10}$$

Equations (8) and (10) are identical to Eq. (3.3) and (3.12) in GSR, even though the series for fixed d are very different in the two cases.

Following GSR, we have also derived the first two terms in the perturbation series in powers of $1/\eta$ for the percolation threshold,

$$p_c = \eta^{-1}[1 + \tfrac{3}{2}\eta^{-1} + \cdots] \ . \tag{11}$$

Our basic conclusion from these calculations is that percolation on the 2-hypercube and in an infinite system are essentially the same in the high-dimension limit. The coincidence of our two terms in $1/\eta$ expansions reflects the irrelevancy of the restriction to linear dimension 2 in the high-dimensional limit. In this limit, each bond that is added to a cluster extends into yet another spatial dimension with probability unity, and this topology can always be embedded on the 2-hypercube. This also explains why the $1/\eta$ expansions of the two problems coincide, to lowest order. The primary difference lies in the reduction of the coordination by one-half, which may be interpreted as the spatial dimension reduced by half. This smaller coordination number implies that the correction to the Bethe approximation is more significant for the hypercube than for an infinite-size system.

In this confined space, the spatial dimension also gives the maximum cluster length d in the Hamming metric. Thus d is the quantity that controls finite-size effects. We will consider the quantitative verification of the finite-dimensional scaling that follows in the next section.

IV. NUMERICAL EVIDENCE FOR FINITE-DIMENSIONAL SCALING

In this section, we analyze both enumeration and Monte Carlo data for $\tilde{n}_s$ in order to test the hypothesis that percolation properties on the hypercube obey finite-*dimensional* scaling, in close analogy with the finite-*size* scaling of systems at the critical point. For this scaling analysis, we supplemented our enumeration results with Monte Carlo data, obtained by adapting the Leath algorithm[16] to generate clusters connected to the origin of a 2-hypercube in spatial dimension $d=10$ and $d=16$. In addition to complementing the enumeration results, the Monte Carlo data allows us to determine the scaling of cluster mass versus length on the hypercube. This mass-length relation will be used to describe the relaxation time of random walks on a given configuration in terms of the cluster mass.

A. At the percolation threshold

At the percolation threshold [Eq. (11)] we postulate that the cluster size distribution, $\tilde{n}_s$, has the scaling form

$$\tilde{n}_s(p=p_c,d)\sim s^{1-\tau}F(s/s_d^*)\ , \tag{12}$$

where $F(s/s_d^*)\rightarrow$const for $s\ll s_d^*$, and $F(s/s_d^*)$ decays faster than any power law for large s/s_d^*. Here s_d^* is the typical cluster size on a 2-hypercube in dimension d at $p=p_c$. This characteristic size is limited by the finite dimensionality of the system. This is analogous to the limitation of the characteristic size in a system of finite linear dimension, which is the basis of finite-size scaling. Since the spatial dimension d now plays a role of a length, we expect that s_d^* will scale as d^{d_f}, where d_f is the fractal dimension describing the relation between cluster mass and length.

In Fig. 1, we illustrate the dimensional crossover, which sets in for $s_d^*\simeq 90$ in $d=10$ and for $s_d^*\simeq 900$ in $d=16$. For $s<s_d^*$, $\tilde{n}_s(p_c,d)$ scales as $s^{1-\tau}$ while for $s>s_d^*$, $\tilde{n}_s(p_c,d)$ decays rapidly. From a Neiville analysis[17] on the enumeration polynomial, we estimate that $1-\tau=-1.38\pm0.02$, -1.44 ± 0.02, -1.48 ± 0.02, and -1.49 ± 0.02 for $d=16$, 20, 30, and 40, respectively. Evidently, $1-\tau$ tends to its mean-field value[18] of -1.5 as the spatial dimension increases.

To estimate the fractal dimension of clusters on the hypercube, we plot the cluster mass versus length, where we use the maximum Hamming distance of each cluster as its length measure (Fig. 2). To interpret the data, it is helpful to classify clusters according to whether or not they contain closed loops, as a power-law relation between mass and length (Hamming distance) appears to hold only for loopless clusters (Fig. 2). For increasing spatial dimension, however, clusters without closed loops form a progressively larger fraction of the total number

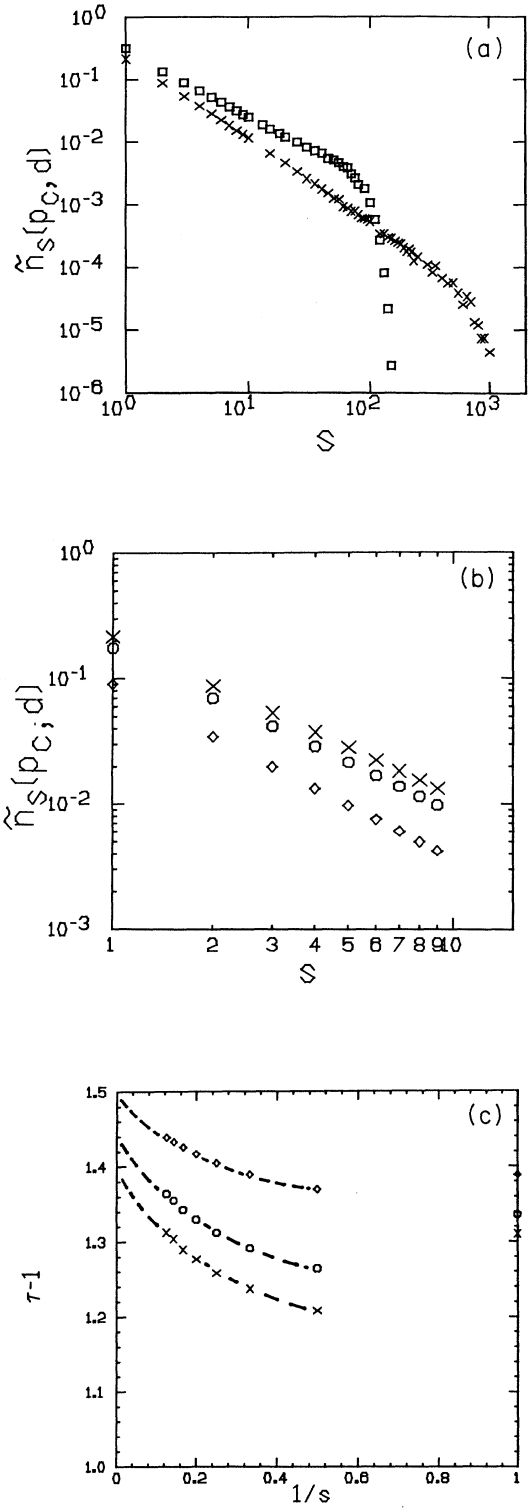

FIG. 1. Double logarithmic plot of $\tilde{n}_s(p_c,d)$ vs s. (a) Monte Carlo data for the cases $d=10$ (□) and for $d=16$ (×) are shown. This data represent averages over 10^5 configurations. Also shown is (b) the enumeration data for $d=16$ (×), 20 (○), and 40 (◇). (c) Slopes between two successive points of (b) vs $1/s$. The dashed lines are to represent the expected behavior for large s.

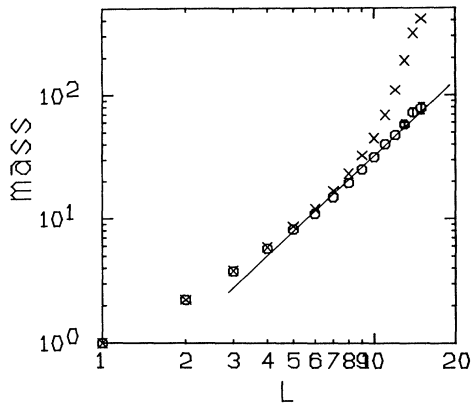

FIG. 2. Plot of the averaged mass vs L on a double logarithmic scale at p_c. The slope means the fractal dimension d_f. Data points are for the cases, including the loop structures (×), and not including the loop structures (○), in $d=16$. Slope 2 is indicated by the straight line.

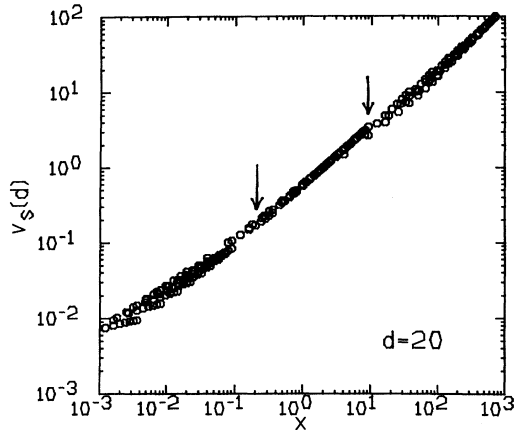

FIG. 3. Plot of $v_s(d)$ vs x on a double logarithmic scale, to check the data collapse for $d=20$. The estimated scaling regime is indicated by arrows.

of clusters (cf. Table I). Consequently, we study only the scaling behavior of the loopless clusters. From this data, we estimate the fractal dimension d_f to be approximately equal to 2 in $d=16$. This accords with the mean-field value, $d_f=4$, when we account for the fact that the Hamming distance is the square of the Euclidean distance. This exponent value supports the hypothesis that percolation clusters in the hypercube and on an infinite lattice are very similar when the spatial dimension is sufficiently large.

B. Above the percolation threshold

Above the percolation threshold, the percolation correlation length ξ, which scales as $\xi\sim\epsilon^{-\nu}$ with $\epsilon\equiv(p-p_c)/p_c$, introduces an additional characteristic size s^* which scales as $s^*\sim\xi^{d_f}\sim\epsilon^{-\nu d_f}$. Therefore, we postulate that the cluster-size distribution obeys the two-variable scaling form

$$\tilde{n}_s(p>p_c,d)\sim s^{1-\tau}G(s/s^*(\epsilon),s/s_d^*)\ . \tag{13}$$

For a fixed spatial dimension d, there now exists a crossover value of ϵ^*, which is determined by $\xi^*\sim(\epsilon^*)^{-\nu}\sim d$. When $\epsilon<\epsilon^*$, the cluster size is limited only by the finite dimensionality d. In this case, the first argument of G can be set to zero, leading to the finite-dimensional scaling statement of Eq. (12). For $\epsilon>\epsilon^*$, the percolation correlation length ξ is smaller than the dimensional correlation length d, and Eq. (13) reduces to the single-parameter scaling statement of conventional percolation.[18] Thus the cluster size distribution scales as $s^{1-\tau}$ for $s<s^*(\epsilon)$, and cut off exponentially fast for $s^*(\epsilon)<s<s_d^*$. However, the cluster size is ultimately limited by s_d^* due to the finite dimensionality of the system so that for $s>s_d^*$ the scaling in s/s^* breaks down.

To test this picture, we plot enumeration data for $v_s\equiv-\ln(\tilde{n}_s/s^{1-\tau})$ versus the scaling variable $x\equiv\epsilon^{1/\sigma}s\sim s/s^*$, where $1/\sigma\equiv\nu d_f$, for the cases $d=20$ in Fig. 3, in which we use the mean-field value $\sigma=\frac{1}{2}$. According to the scenario described above, there exists a range of x for which data collapsing holds. In fact we observe three distinct regimes, with data collapsing occurring only for $x^*\le x\le x_d^*$. In this intermediate "scaling" regime, the scaling function varies exponentially in s/s^*. When $x>x_d^*$, the "compact regime," data collapsing breaks down, but $\tilde{n}_s$ is still an exponentially damped function of s/s_d^*. However for $x<x^*$, $\tilde{n}_s$ follows a power-law behavior.

To determine the functional form of the scaling function in the scaling regime $G(s/s^*,s/s_d^*)$ we plot v_s versus s in Fig. 4 on a double logarithmic scale, for several values of ϵ. In this plot, we expect a crossover between the power-law regime to the scaling regime to occur when $s^*(\epsilon)\sim\epsilon^{-1/\sigma}$, which should be observable for small ϵ. This behavior is suggested by the data shown in Fig. 4. For $\epsilon=0.01$ the points appear to lie on a horizontal line, indicative of power-law behavior. However for larger ϵ, the data points appear to fall on a line of nonzero slope, suggesting that

$$\tilde{n}_s\sim s^{1-\tau}\exp[-(\epsilon^{1/\sigma}s)^n]\ . \tag{14}$$

By computing the slope of the straight line that passes through two successive data points in Fig. 4, and plotting these successive slopes versus $1/s$, we determine the exponent n (Fig. 5). Even for the case $\epsilon=1.0$, for which the data are linear to the eye, the successive slopes change

TABLE I. Compared are dimensional dependences for (1) number of configurations with closed loops among 10^4 configurations, (2) average number of branches, and (3) fraction of mass in side branches. The quantities (2) and (3) are averaged over configurations with loopless clusters.

	$d=10$	$d=13$	$d=16$	$d=18$
(1)	3434	2804	2350	2228
(2)	2.49±0.026	2.57±0.029	2.70±0.035	3.04±0.054
(3)	0.35±0.008	0.34±0.008	0.35±0.008	0.42±0.012

continuously with $1/s$. For $d=16$, the slope increases monotonically as $1/s$ decreases for $\epsilon=1,3,5$. However for $\epsilon=8$, the slopes do not always increase, and by $\epsilon=9$, the slopes actually decrease. This change indirectly suggests the occurrence of the second crossover behavior from scaling to compact regime which arises for large ϵ. That the slopes change continuously with s means Eq. (14) does not hold precisely in finite dimension. But as we can observe in Fig. 5, the total range of slopes over the entire range of s ($s \leq s_d^*$) becomes smaller as ϵ or dimension becomes larger. Eventually in the limit $d \to \infty$, the slopes for each two successive points are independent of cluster mass s. Therefore for large dimension, Eq. (14) is relevant to describe the probability $\tilde{n}_s$.

The value of the exponent n in Eq. (14) is known as the Kunz and Souillard formula[19] to be $1-1/d$, for the infinite linear size case. However, when the cluster is bounded, we do not expect the Kunz and Soulillard formula to be valid. In Fig. 5(a), we cannot extrapolate reliably to the $1/s \to 0$ limit, because the cluster size is bounded. Hence even for the case $\epsilon=1$ in $d=16$, we estimate the slope to increase up to ~ 0.9 for large size clusters. But if we extrapolate up to the $1/s \to 0$ limit, the slope is expected to be $1-1/d=0.9375$ in $d=16$, the Kunz and Souillard value.

In summary, there are three regimes of behavior for $\tilde{n}_s(d)$ in finite spatial dimension above p_c. When p is very close to p_c, $\tilde{n}_s(d)$ decays as a power law. In the intermediate regime, defined by the region between the two arrows in Fig. 3, $\tilde{n}_s(d)$ is described approximately by the scaling function, Eq. (14), with an exponent n that depends on dimension. On the other hand, when p is near 1, there is a second crossover to a regime where percolation clusters are compact and homogeneous.

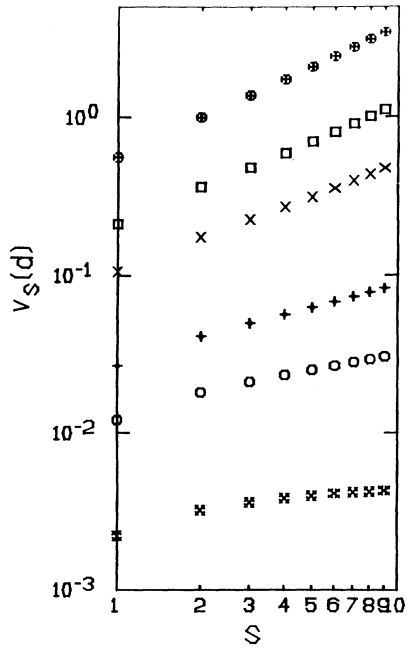

FIG. 4. Plot of $v_s(d)$ vs s on a double logarithmic scale, to check the formula Eq. (14). The slope of the straight line means the exponent n. Data points are in $d=20$ for $\epsilon=0.01, 0.05, 0.1, 0.3, 0.5, 1.0$ from the bottom.

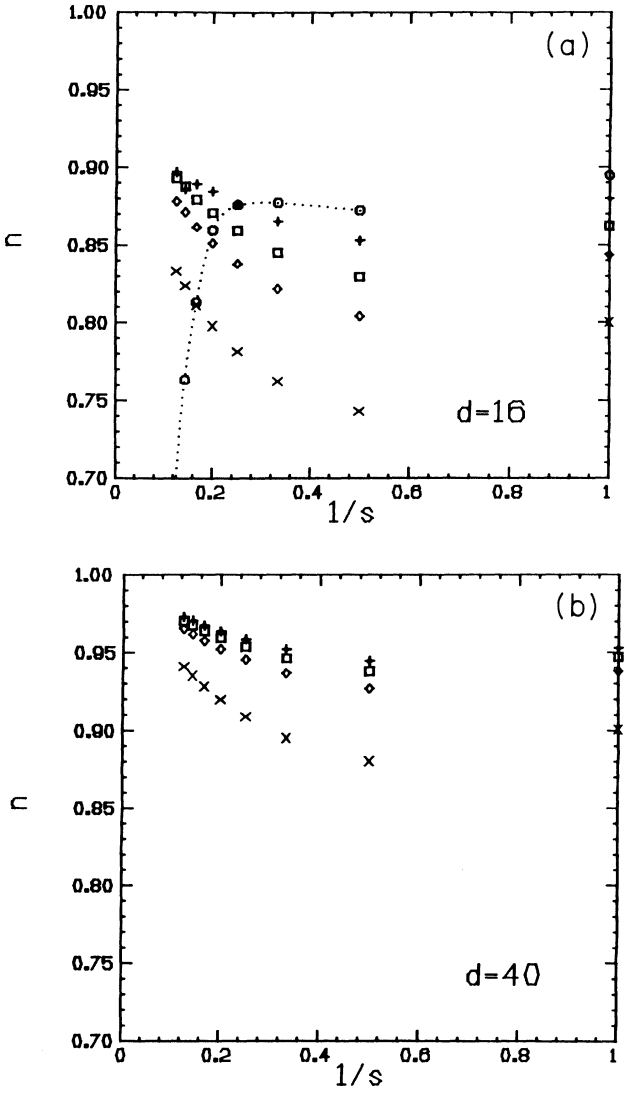

FIG. 5. Plot of slopes between each two successive points vs $1/s$ (a) for $\epsilon=1,3,5,8,9$ in $d=16$ from the bottom and (b) for $\epsilon=1,3,5,8$ in $d=40$.

V. RANDOM WALKS ON ONE-DIMENSIONAL PERCOLATION CLUSTERS

As a preliminary to understanding the relaxation of random walks on percolation clusters embedded in the hypercube, we first consider the relaxation of a random walk on a finite interval of length L. In the continuum limit, the random walk obeys the diffusion equation

$$\frac{\partial P(x,t)}{\partial t} = D\nabla^2 P(x,t) , \tag{15}$$

where $P(x,t)$ is the random-walk probability density at position x and time t, and D is the diffusion coefficient.

We must solve this equation for the initial condition in which a random walker starts at $x=l$ with reflecting boundary conditions at the ends of the interval, i.e., $\partial P/\partial x=0$ at $x=0$ and $x=L$. By standard methods, the solution is

$$P(x,t)=\frac{1}{L}+\frac{2}{L}\left[\frac{L-1}{L}\right]\sum_{n=1}^{\infty}\cos\frac{n\pi x}{L}\cos\frac{n\pi l}{L}\times e^{-D(n\pi/L)^2 t}. \quad (16)$$

Thus the probability density relaxes to its equilibrium value at an exponential rate.

Next consider the mean of the absolute value of the displacement of the random walk from its starting point, averaged over all random-walk trajectories

$$\langle r(t)\rangle_l=\int_0^l (l-x)P(x,t)dx+\int_l^{L-l}(x-l)P(x,t)dx\ , \quad (17)$$

where the subscript denotes that the initial position of the walk is at $x=l$, and the angle brackets denote an average over all random-walk trajectories (see Fig. 6). After averaging over initial positions, the asymptotic decay of $\langle r(\infty)\rangle-\langle r(t)\rangle$ is given by

$$\langle r(\infty)\rangle-\langle r(t)\rangle\sim\frac{2(L-1)}{\pi^2}\exp\left[-D\frac{\pi^2}{L^2}t\right]. \quad (18)$$

Note that the characteristic time of this decay varies as the square of the interval length.

A stretched exponential decay occurs when one averages Eq. (18) over a suitable distribution of interval lengths L. For example, in one-dimensional percolation, the probability to have an interval of length L equals $p^L(1-p)^2$. Thus by averaging over this distribution, we find

$$\overline{\langle r(\infty)\rangle-\langle r(t)\rangle}\sim\frac{2(1-p)^2}{\pi^2}\int_0^{\infty}e^{-cL}(L-1)e^{-D(\pi^2/L^2)t}dL\ , \quad (19)$$

where $c=-\ln p$, so that $c\sim(p_c-p)$ for $p\simeq 1$. Here the overline denotes the average over all interval lengths. Using the steepest-descent method, we thereby obtain

$$\overline{\langle r(\infty)\rangle-\langle r(t)\rangle}\sim(p_c-p)^{-1}t^{1/2}\exp[-(t/\mathcal{T})^{1/3}]\ , \quad (20)$$

with $\mathcal{T}=(p_c-p)^{-2}$. The relaxation exhibits stretched exponential decay with an exponent $\frac{1}{3}$, and a characteristic time $\mathcal{T}$ that diverges as $(p_c-p)^{-2}$. The exponent value of $\frac{1}{3}$ is a characteristic feature of the one-dimensional nature of the system.

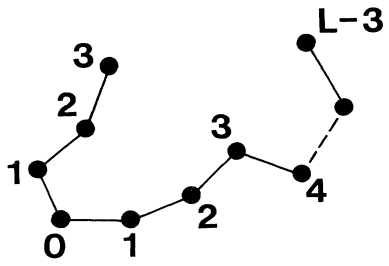

FIG. 6. Schematic picture for the metric used in Sec. V on a one-dimensional chain with length L.

VI. RANDOM WALKS ON PERCOLATION CLUSTERS IN THE HYPERCUBE

The relaxation of random walks on the hypercube depends on the structure of percolation clusters in this system. In Sec. IV, we have argued that these percolation clusters are self-similar near the percolation threshold, but with a structure which resembles that of clusters on the Bethe lattice, namely clusters are ramified and highly branched. According to our Monte Carlo data, the number of side branches and the mass fraction in the side branches are both increasing functions of dimension (cf. Table I). Thus clusters cannot be regarded as quasi-one-dimensional, and this feature is an essential ingredient in our description of the relaxation of random walks on the hypercube.

Due to the correspondence between percolation clusters on the hypercube and on the Bethe lattice, the fractal dimension of a random walk is $d_w=3$ (according to our use of the Hamming distance as the metric), rather than the value $d_w=2$ which is appropriate for one dimension.[20,21] Employing a characteristic time scaling as L^{d_w} with $d_w=3$, the leading behavior of the relaxation of the mean displacement to its equilibrium value is given by

$$\langle r(\infty)\rangle-\langle r(t)\rangle\sim L\exp(-t/L^{d_w})\ , \quad (21)$$

with $d_w=3$.

We now average Eq. (21) over all cluster configurations. In the self-similar regime, the cluster size distribution is most conveniently expressed as a function of cluster mass, rather than in terms of a length scale. Hence we use the relation $L\sim s^{1/d_f}$ where L is the maximum Hamming distance of the cluster, to rewrite Eq. (21) as

$$\langle r(\infty)\rangle-\langle r(t)\rangle\sim s^y\exp(-t/s^{\alpha})\ , \quad (21')$$

where $\alpha=d_w/d_f$ and $y=1/d_f$. Using the cluster-size distribution, Eq. (14), the configurational average of the relaxation function now becomes

$$\overline{\langle r(\infty)\rangle-\langle r(t)\rangle}\sim\int_0^{s_{\max}}s^{1-\tau}\exp(-\epsilon^{n/\sigma}s^n)s^y\exp(-t/s^{\alpha})ds \quad (22)$$

with $\epsilon=(p-p_c)/p_c$. In the limit of the spatial dimension becoming large, the upper limit of the integral can be regarded as infinite. Now using the steepest-descent method, Eq. (22) yields

$$\overline{\langle r(\infty)\rangle-\langle r(t)\rangle}\sim\epsilon^{-\alpha}t^{-x}\exp[-(t/\mathcal{T})^{\beta}]\quad(p\to p_c)\ , \quad (23)$$

where

$$\beta=\frac{n}{n+\alpha}\ ,$$
$$\mathcal{T}\sim(p-p_c)^{-\alpha/\sigma}\ ,$$
$$a=\frac{n(4-2\tau+2y+\alpha)}{2\sigma(n+\alpha)}\ , \tag{24}$$
$$x=\frac{1}{2}-\frac{y+3-\tau}{n+2}\ .$$

We consider the infinite-dimensional case, which corresponds to the thermodynamic limit. Thus substituting the mean-field values $d_f=2$, $d_w=3$, $\tau=\frac{5}{2}$, $\sigma=\frac{1}{2}$, $n=1$ into Eqs. (24), we find

$$\overline{\langle r(\infty)\rangle-\langle r(t)\rangle}\sim(p-p_c)^{-3/5}t^{-1/6}\exp[-(t/\mathcal{T})^{2/5}] \quad (p\to p_c)\ , \tag{25}$$

with $\mathcal{T}\sim(p-p_c).^{-3}$

At the percolation threshold, the absence of a cutoff in the cluster size function in Eq. (22) now leads to

$$\overline{\langle r(\infty)\rangle-\langle r(t)\rangle}\sim t^{-x'}\quad (p=p_c)\ , \tag{26}$$

with

$$x'=\frac{\tau-y-2}{\alpha}\ . \tag{27}$$

The exponent x' turns out to equal zero when the mean-field values of the exponent τ, y, α are used. The value x' is close to the value by Ogielski, $x_{SG}(T_g)=0.065\pm0.005$. Hence the relaxation at the critical temperature (probability) is extremely slow.[22] Since x' may actually be equal to zero, we need to consider the next order term in the saddle-point calculation. So there might be some possibility to have a different functional form from power-law relaxation at p_c. The way to derive the stretched exponential decay is basically the same as the one used in Ref. 12 except for the following. In the reference, the percolation clusters are regarded as quasi-one-dimensional, so that they used $d_w=2$, but we proved $d_w=3$ is correct. Finally it is worthwhile to note that the stretched exponential behavior derived above is very relevant in the long time limit, because we used the ground-state energy of the characteristic times in Eq. (21).

A. A comparison to the simulations of Ogielski

Let us compare our numerical values with the ones in the Ising spin-glass system obtained by Ogielski.[6] We first notice that Eq. (25), which corresponds to $q(t)$, has the same functional form as the Ogielski's empirical formula. In the spin-glass system, the exponents x and β depend on temperature. Since Eq. (25) was obtained near the percolation threshold, it is natural to compare our result with the relaxation function of a spin glass near the critical point, the glassy temperature. Numerical values seem to be consistent with the numerical estimation of the simulation data as near the critical temperature[6] that the exponents x,β are very "roughly" $x\sim0.1$ and $\beta\sim0.4$.

This stretched exponential behavior is expected to occur only in the scaling regime near the percolation threshold. In the compact regime sufficiently above p_c, the random-walk relaxation follows a pure exponential decay, which was proved analytically by Campbell *et al.*[11] Consequently, it is natural to expect that estimates for the exponent β which are based on a numerical approach will decay monotonically from $\beta=1$ to $\beta\sim0.4$ in the large-dimensionality limit, as probability p decreases from 1 to near p_c. A sharp transition is expected to happen across the boundary of the two different regimes, the scaling regime and the compact regime.

Next we define dynamic exponent z in the random-walk problem as $\mathcal{T}\sim(p-p_c)^{-z\nu}$. Since $z\nu=3$ from Eq. (25), we obtain the dynamic exponent z to be 6 with the mean-field value $\nu=\frac{1}{2}$ in the Euclidean metric. The dynamic exponent value $z=6$ accidentally coincides with z_{SG} for the spin-glass system obtained by Ogielski. From the above numerical comparison between the random-walks model and the spin-glass model, we could say that the random-walk model illustrates well the relaxation of the Ising spin-glass system.

B. A comparison to the simulations of Campbell *et al.*

Next let us compare our results with the numerical simulations of Campbell *et al.* In their work, simulations were performed in dimensions $d=10$, 14, 16, 17 and data were presented for $d=16$. However, the situation of interest is the limit of $d\to\infty$, and they do not provide a systematic way of extrapolating their results to this limit. In particular, the exponent n in the cluster size distribution of Eq. (14) has an apparent size dependence for spatial dimension $d=16$ (cf. Fig. 5). This variation feeds in to the apparent value of β that would be observed in the random-walk relaxation. Furthermore, the simulation of Campbell *et al.* was apparently performed on the "largest" percolation clusters. This selection is desirable in order that the correct cluster size distribution for large clusters follow the cluster size distribution formula Eq. (14) more reasonably. Nevertheless, percolation clusters have to be selected randomly in the scaling regime in order to have a variety of characteristic times. Thus the stretched exponential distribution can be obtained by averaging over many characteristic times. An additional source of discrepancy is that the value of percolation threshold employed by Campbell *et al.* is somewhat greater than the value given by the high-dimensional expansion of Eq. (11) in $d=16$. Hence the relaxation they observe is rather a behavior characteristic of p slightly above p_c. These difficulties would be playing a lesser role in larger spatial dimension. Nevertheless, in order to compare to their data, we exploit the fact that the spectral dimension depends on dimension very weakly (Alexander-Orbach conjecture)[23]. Hence if we plug $\alpha=\frac{3}{2}$ into Eq. (24), then the exponent β is only a function of the exponent n. We estimate the value to be $n=0.85\sim0.9$ in $d=16$ for the large size cluster from Fig. 5. Using the estimated value of n, we obtain $\beta=0.362\sim0.375$, which is comparative to the value $\beta\sim\frac{1}{3}$ obtained by Campbell *et al.* But when dimension is very large, which is in the thermodynamic limit, we expect that $\beta=0.4$ for $p\to p_c^+$.

VII. CONCLUSIONS

We have investigated the structure of percolation clusters on a hypercube of linear dimension 2 and the dynamics of random walks on these percolation clusters, in order to study the relaxation of an Ising spin glass. We employ the exact enumeration method to obtain the cluster size distribution of the percolation clusters. The perimeter polynomials are derived for general dimension up to ninth order. Based on numerical values of the exact enumeration polynomials, we find that above the percolation threshold, a crossover from scaling to compact behavior occurs in a finite range of p. The dimensional dependent behavior of the crossover is explained by introducing the finite-dimensional scaling argument. Since the coordination number is d in a d-dimensional hypercube instead of $2d$, it is likely that percolation clusters in a d-dimensional hypercube resemble the ones in a $(d/2)$-dimensional hypercubic lattice of infinite-dimensional limit; the percolation cluster in a hypercube is reduced to the one on the Bethe lattice.

We obtained the configuration-averaged mean displacement of random walks on the percolation clusters, which shows (1) a stretched exponential relaxation as $(p-p_c)^{-a}t^{-x}\exp[-(t/\mathcal{T})^{\beta}]$ where $\mathcal{T}\sim(p-p_c)^{-z\nu}$ $p\to p_c^{+}$ with the exponents $a\sim\frac{3}{5}$, $x\sim\frac{1}{6}$, $\beta=\frac{2}{5}$, $z\nu=3$ in the long time limit, and shows (2) a tendency of extremely slow relaxation at $p=p_c$. These results give a good illustration for Ogielski's empirical formula and numerical data. Besides Ogielski's empirical formula, our result includes the behavior of the amplitude which diverges as $(p-p_c)^{-a}$. We noticed in Ogielski's paper that amplitude decreases with increasing temperature. But the detail divergent behavior cannot be checked with the data appearing in the paper.[6] The temperature (probability) dependent behavior for the exponents x and β can be understood from the transition behavior of the cluster size distribution from the compact to scaling regime. Finally we compare our prediction with the numerical simulation performed by Campbell *et al.* Due to the memory space limitation, they performed in relatively low dimension, in which theoretical prediction is not expected to be good. The numerical results are in agreement only qualitatively with our prediction. We do not agree with Campbell's conclusion that the relaxation shows the stretched exponential with exponent $\beta=\frac{1}{3}$ at the percolation threshold. Instead we showed that the relaxation is of critical slowing down at the percolation threshold.

Note added. The $1/d$ expansion has also been performed to investigate the phase structure of the Ising spin glass on a hypercubic lattice recently.[24]

ACKNOWLEDGMENTS

I would like to thank Professor S. Redner and C. L. Henley for helpful discussions. The Center for Polymer Studies is supported in part by grants from the ARO, NSF, and ONR. This financial support is gratefully acknowledged. Also I acknowledge support in part from the Regents of the University of California.

APPENDIX

The perimeter polynomials $\tilde{D}_s(p,d)\equiv s\sum_t g_{st}(1-p)^t$ for general dimension d:

$$\tilde{D}_1(p,d)=q^d\,,$$

$$\tilde{D}_2(p,d)=q^{2d-2}\begin{bmatrix}d\\1\end{bmatrix}\,,$$

$$\tilde{D}_3(p,d)=q^{3d-4}\left[3q^{-1}\begin{bmatrix}d\\2\end{bmatrix}\right]\,,$$

$$\tilde{D}_4(p,d)=q^{4d-6}\left[q^{-2}\begin{bmatrix}d\\2\end{bmatrix}+(12q^{-2}+4q^{-3})\begin{bmatrix}d\\3\end{bmatrix}\right]\,,$$

$$\tilde{D}_5(p,d)=q^{5d-8}\left[30q^{-4}\begin{bmatrix}d\\3\end{bmatrix}+(60q^{-3}+60q^{-4}+5q^{-6}\begin{bmatrix}d\\4\end{bmatrix}\right]\,,$$

$$\tilde{D}_6(p,d)=q^{6d-10}\left[21q^{-6}\begin{bmatrix}d\\3\end{bmatrix}+(72q^{-4}+216q^{-5}+324q^{-6}+36q^{-7})\begin{bmatrix}d\\4\end{bmatrix}\right.$$
$$\left.+(360q^{-4}+720q^{-5}+90q^{-6}+120q^{-7}+6q^{-10})\begin{bmatrix}d\\5\end{bmatrix}\right]\,,$$

$$\tilde{D}_7(p,d)=q^{7d-12}\left[7q^{-8}\begin{bmatrix}d\\3\end{bmatrix}+(756q^{-7}+861q^{-8}+238q^{-9})\begin{bmatrix}d\\4\end{bmatrix}\right.$$
$$+(1260q^{-5}+3360q^{-6}+5670q^{-7}+2100q^{-8}+1260q^{-9}+70q^{-11})\begin{bmatrix}d\\5\end{bmatrix}$$
$$\left.+(2520q^{-5}+8400q^{-6}+3150q^{-7}+2100q^{-8}+420q^{-9}+210q^{-11}+7q^{-15})\begin{bmatrix}d\\6\end{bmatrix}\right]\,,$$

$$\tilde{D}_s(p,d)=q^{8d-14}\left[q^{-10}\begin{bmatrix}d\\3\end{bmatrix}+(2676q^{-10}+920q^{-11}+40q^{-12})\begin{bmatrix}d\\4\end{bmatrix}\right.$$
$$+(2400q^{-6}+5760q^{-7}+17\,160q^{--8}+29\,520q^{-9}+22\,080q^{-10}+7440q^{-11}+1240q^{-12}$$
$$+480q^{-13})\begin{bmatrix}d\\5\end{bmatrix}$$
$$+(17\,280q^{-6}+66\,240q^{-7}+97\,920q^{-8}+70\,560q^{-9}+36\,720q^{-10}+12\,960q^{-11}$$
$$+2520q^{-12}+2880q^{-13}+120q^{-16})\begin{bmatrix}d\\6\end{bmatrix}$$
$$\left.+(20\,160q^{-6}+100\,800q^{-7}+75\,600q^{-8}+38\,640q^{-9}+20\,160q^{-10}+5600q^{-12}\right.$$
$$\left.+840q^{-13}+336q^{-16}+8q^{-21})\begin{bmatrix}d\\7\end{bmatrix}\right],$$

$$\tilde{D}_9(p,d)=q^{9d-16}\left[(4464q^{-13}+441q^{-14})\begin{bmatrix}d\\4\end{bmatrix}+(5400q^{-8}+27\,540q^{-9}+62\,370q^{-10}+111\,240q^{-11}\right.$$
$$+122\,355q^{-12}+63\,990q^{-13}+16\,740q^{-14}$$
$$+1980q^{-15}+585q^{-16})\begin{bmatrix}d\\5\end{bmatrix}$$
$$+(71\,280q^{-7}+281\,880q^{-8}+579\,150q^{-9}+848\,880q^{-10}+793\,800q^{-11}$$
$$+498\,960q^{-12}+189\,000q^{-13}+63\,990q^{-14}+23\,220q^{-15}+5400q^{-16}$$
$$+405q^{-17}+1080q^{-18})\begin{bmatrix}d\\6\end{bmatrix}$$
$$+(226\,800q^{-7}+1\,270\,080q^{-8}+2\,018\,520q^{-9}+1\,884\,330q^{-10}$$
$$+1\,084\,860q^{-11}+640\,710q^{-12}+120\,960q^{-13}+144\,585q^{-14}+34\,020q^{-15}$$
$$+5670q^{-16}+3780q^{-17}+5670q^{-18}+189q^{-22})\begin{bmatrix}d\\7\end{bmatrix}$$
$$+(181\,440q^{-7}+1\,270\,080q^{-8}+1\,587\,600q^{-9}+846\,720q^{-10}+635\,040q^{-11}$$
$$+52\,920q^{-12}+141\,120q^{-13}+52\,920q^{-14}+2520q^{-16}+10\,584q^{-17}+1512q^{-18}$$
$$\left.+504q^{-22}+9q^{-28})\begin{bmatrix}d\\8\end{bmatrix}\right].$$

---

*Present address.

[1]P. C. Hohenberg and B. I Halperin, Rev. Mod. Phys. **49**, 435 (1977).

[2]R. G. Palmer, D. L. Stein, E. Abrahams, and P. W. Anderson, Phys. Rev. Lett. **53**, 958 (1984).

[3]M. Randeria, J. P. Sethna, and R. G. Palmer, Phys. Rev. Lett. **54**, 1321 (1985).

[4]D. Dhar and M. Barma, J. Stat. Phys. **22**, 259 (1980).

[5]H. Sompolinksy and A. Zippelius, Phys. Rev. B **25**, 6860 (1982).

[6]A. T. Ogielski, Phys. Rev. B **32**, 7348 (1985).

[7]J. E. Martin and J. P. Wilcoxon, Phys. Rev. Lett. **61**, 373 (1988).

[8]B. Y. Balagurov, and V. G. Vaks, Zh. Eksp. Teor. Fiz. **65**, 1939 (1974) [Sov. Phys.—JETP **38**, 968 (1974)]; P. Grassberger and I. Procaccia, J. Chem. Phys. **77**, 6281 (1982); K. Kang and S. Redner, Phys. Rev. A **32**, 435 (1985).

[9]K. Gunnarsson, P. Svedlindh, P. Nordblad, L. Lundgren, H. Aruga, and A. Ito, Phys. Rev. Lett. **61**, 754 (1988).

[10]S. Kirkpatrick and D. Sherrington, Phys. Rev. B **17**, 4384 (1978).

[11]I. A. Campbell, J. M. Flesselles, R. Jullien, and R. Botet, J. Phys. C **20**, L47 (1987); Phys. Rev. B **37**, 3825 (1988).

[12]A. J. Bray and G. J. Rodgers, Phys. Rev. B **38**, 11461 (1988).

[13]S. Redner, J. Stat. Phys. **29**, 309 (1982).

[14]D. S. Gaunt, M. F. Sykes, and H. Ruskin, J. Phys. A **9**, 1899 (1976).

[15]M. Fisher and D. S. Gaunt, Phys. Rev. **133**, A224 (1964).

[16]P. L. Leath, Phys. Rev. B **14**, 5064 (1976).
[17]D. S. Gaunt and A. J. Guttmann, in *Phase Transitions and Critical Phenomena,* edited by C. Domb and M. S. Green (Academic, New York, 1974), Vol. 3.
[18]D. Stauffer, *Introduction to Percolation Theory* (Taylor and Francis, London, 1985).
[19]H. Kunz and B. Souillard, J. Stat. Phys. **19**, 77 (1978).
[20]B. Kahng and S. Redner, J. Phys. A **22**, 887 (1989).
[21]S. Havlin, J. E. Kiefer, and G. H. Weiss, Phys. Rev. A **35**, 1403 (1987).
[22]R. B. Griffiths, Phys. Rev. Lett. **23**, 17 (1969).
[23]S. Alexander and R. Orbach, J. Phys. (Paris) **43**, L625 (1982).
[24]A. Georges, M. Mezard, and J. S. Yedidia, Phys. Rev. Lett. **64**, 2937 (1990).